

H-Spar: Framework Model for Efficient Land-Use Classification using Hybrid Features and Coarse to Fine Sparselets

P. Dolphin Devi, K. Chitra

Abstract: Land-use (LU) classification is a challenging field in Remote Sensing (RS) and in quantitatively estimating the impact of human involvement on natural resources. This LU classification covers wide range of application in natural resource management and ability to understand the human modification. Defining and extraction of feature and classification approaches may pose new challenges for researchers. Thus, this paper proposed hybrid feature extraction namely Sparse Principal Component Analysis with Pyramid Histogram of Oriented Gradients (SPCA-PHOG) for land use classification. Furthermore spatial pattern based classification is introduced than even before. In this research paper, an innovative technique of "sparselets" with hybrid feature extraction (H-Spar) is presented which is based on efficient midlevel visual elements for land-use classification. This element is used to represents an image with huge number of part detectors rather than low level image attributes. If the part detectors increases with images, it will leads to computational complexity problem. To solve is issue, novel training framework is introduced, is represented by with huge number of part detectors namely "sparselets". This proposed hybrid feature extraction and sparselets based classification estimated on datasets and compared with existing approaches.

Index Terms: Land Use, Partlets, Sparseletes, SPCA, HOG.

I. INTRODUCTION

Land-use classification plays a significant role in global change research. It covers wide range of application of natural hazard detection [1], land-use/land-cover (LULC) identification and object detection [12] and vegetative type mapping [14], etc. In the past periods, although important efforts have been developed in various image feature extraction and classification techniques to gather land usage from satellite images, the effective clarification of these satellite images remains one of the most challenging issues faced for remote sensing image study.

Land-use and land-cover classification are two main intrinsic significant in remote sensing. Land-cover contains mainly on its nature belongings and it is the unnaturally reflection of various components in global surface enclosed with natural form or manual creation. Nevertheless, Land-use, containing more on land's public properties, is the output of modernization activities that human implements a serial of biologic, technologic measure to achieve and control the land frequently and periodically. Land-use is the most straight and foremost factor to the land-cover transformation. Research and investigation area in application of Land-use and Land-cover classification on remote sensing, the identical classification structure is typically built up by combining the

two ideas under one scheme, which is named as Remote Sensing Land-Cover/Land-Use classification scheme. There are numerous approaches that have been established to execute the Land-Cover/Land –Use Classification mainly for multispectral and hyperspectral imagery.

Earlier works [5]–[11], [13] mostly focus on classifying pixels or superpixels into their thematic class by using low-level image features (e.g., the texture attributes [6], [13], attributes of colors [5], spatial and temporal attributes [7], [8], or their hybrids methods [9]–[11]) for remote sensing data classification. For instance, a new system for classify the complex object based on texture features was used in [13], for harbors and golf classification. An improved color structure features based satellite image was segmented and classified by SVM classifier in [5]. A novel method via a kernel representation of each pixel based hyperspectral image classification is proposed in [8] with spatial and spectral feature attributes.

The above-mentioned approaches have proved their exciting performance for a minimum number of classes; though, pixels, or even superpixels are caring semantic meanings, which strictly limits the existing image representation methods. Previous classification methods are based on pixel or superpixel level for automatic identification land use and land cover, but these are not enough for real time applications. With the fast growth of remote sensing technology, developments in the spatial resolution of optical sensors exposed unique opportunities for enhancing the field of land-use classification. In specific, scene level image classification using very high resolution(VHR) has more attraction in now a days rather than pixel or superpixel level approaches [2]–[4], [15], [16].

A new approach for land-use classification using scene level is called as bag of visual words (BOVW) model [17] and its alterations [1], [3], [4]. The BOVW model uses local features (SIFT features [18]) from each image, quantize it to a set of visual words, and finally estimate histogram for individual scene classification. This approach yields false classification whenever spatial variations are occurring on images. To overcome these issues, enhanced BOUV model was proposed [19], by which an image is partitioned into spatial sub portions and histogram features are calculated from every sub portions with spatial pyramid matching (SPM) kernel. This method is further extended by using the relative spatial arrangement of visual words from an image, namely spatial

co-occurrence kernel [3], and a spatial pyramid co-occurrence kernel (SPCK) [4]. Furthermore, low level features are extended by unsupervised feature learning method [2] by encoding low level features into pre-learning basis function set. In [15], land use classification performance was enhanced by novel approach of multi feature joint sparse coding (MFJSC) with spatial information.

From this observation, we motivated a new idea for effective classification of land-use using part detector concept. This is to be noted that classification using library that is called partlets(Part Detector). This part detector can used as basic image representation and extract midlevel visual attributes that are more effective than low level visual word concept [1],[3],[4],[17] and it is easier to identify the high level object from an image [20], [21]. In this land-use classification approach, mid-level features are used to represent an image rather than using individual pixel, than features are combined to a large number of pretrained vectors named as part detector. This novel image representation could extract high level content of the image; it is more suitable for complex real world land-use image classification.

Extension of HOG method is introduced in human detection for successful evaluation of HOG. The most successful work of human detection is performed in [22] using HOG feature extraction. An improved pyramid HOG descriptor is used to characterize local shape features at different spatial scale to identify human actions [23]. This pyramid HOG is using pyramid decomposition method to represent human shape at different angle. Gradient method for human detection with Haar wavelets features based on SVM classifier is proposed in [24]. This method is having part descriptors to identify the different parts occlusion of human activity. Human smile recognition can be performed with novel features of PHOG rather than Gabor features [25]. These demonstrated shows the PHOG features with shorter vector length could achieve a higher performance with low computational time.

The paper is organized as follows. Hybrid feature extraction and the partlets-based land-use classification method are introduced in Section II. Section III defines comparative experimental results. As a final point, conclusions are discussed in Section IV.

II. PROPOSED METHODOLOGY

In this paper, the hybrid feature extraction and part detector based classification is performed for land-use classification. The detail description of this flow is discussed in this section and flow is explained in Fig 1.

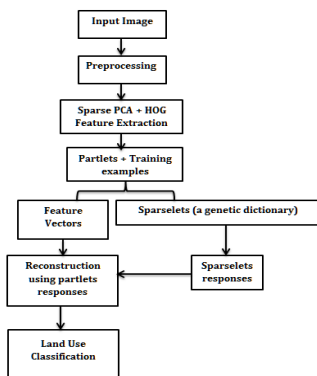


Fig 1. The Flow of our proposed model

2.1 Feature Extraction

Our proposed model was experimented by hybrid feature extraction of PHOG and Sparse PCA on satellite images and the short description as follows.

2.1.1 Sparse PCA

Regression form of Principle Component Analysis (PCA) is called sparse PCA. Consider a training sample of a given dataset as $X = \{x_i\}_{i=1}^n$ in R^p . Let assume the column of X are all zero. Singular Value Decomposition is used to decompose X in PCA.

$$X = UDV^T \tag{1}$$

Where

$Z = UD$, Represents the principle components (PC's)

U = Eigen Matrix

This is to be noted that each important features of data can be represented by linear combination of p variables in each PC's. In [3] proposed a self-constrained regression criterion to derive PC's.

Let i^{th} row of the input matrix X , can be defined as x_i . Let $\alpha = [\alpha_1, \alpha_2, \dots, \alpha_k]^T$ and $\beta = [\beta_1, \beta_2, \dots, \beta_k]^T$.

For any $\lambda > 0$, let

$$\begin{aligned} (\hat{\alpha}, \hat{\beta}) = & \arg \min_{\alpha, \beta} \sum_{i=1}^n \|x_i - \alpha\beta^T x_i\|^2 + \lambda \sum_{j=1}^k \|\beta_j\|^2 \quad \text{subject to } \|\alpha\|^2 = I_k \\ \end{aligned} \tag{2}$$

Then $\hat{\beta}_j \propto V_j$ for $j=1,2,3,..,k$.

Sparse loading is obtained by adding lasso penalty into equation (2), and these equations are optimized as

$$\begin{aligned} (\hat{\alpha}, \hat{\beta}) = & \arg \min_{\alpha, \beta} \sum_{i=1}^n \|x_i - \alpha\beta^T x_i\|^2 + \lambda \sum_{j=1}^k \|\beta_j\|^2 + \sum_{j=1}^k \lambda_{1,j} \|\beta_j\| \\ \end{aligned} \tag{3}$$

subject to $\alpha^T \alpha = I_k$.

Where the similar λ value is used for all k components, $\lambda_{1,j}$ is permitted for correcting the value of j PCs. The above discussed optimization problem is an elastic net problem. By selecting suitable λ and $\lambda_{1,j}$, we find sparse vector β_j . basically λ is selected to be a small positive number to overcome potential col-linearity problems in X . Let us assume a fixed value of λ in Equation (3), can be solved by using the LARS-EN algorithm [26].

2.1.2 PHOG

In current evaluation, PHOG is used as a spatial based shape descriptor, which is applied on image for classification [27]. PHOG descriptor characterizes the spatial property of image edges and transformed it into vector. This descriptor is mostly stimulated by two bases: (1) pyramid representation [28], and (2) the Histogram of Oriented Gradients (HOG) [29].

In this research work, PHOG features are extracted from the edge of the land-use region. Here local features were taken by distributing edge orientation over an image and spatial details are extracted by tilting an image into sub region at various resolutions. The procedures of extracting features from land-use region using PHOG are as follows.

Step 1: First, an input image is applied to edge detection process using canny edge detector. It represents the shape features of an image.



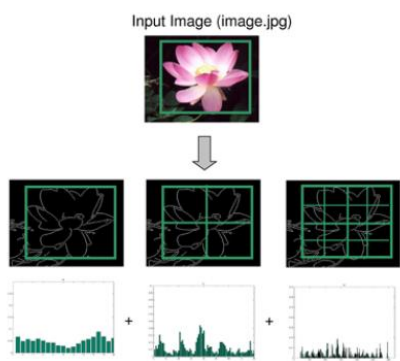


Fig 2: PHOG Feature extraction from an image

Step 2: Second, the image is divided into multiple pyramid level. As shown in Fig 2, the grid at level “1” has 2^1 cells along every dimension.

Step 3: In each pyramid level of all grids has been undergone for HOF feature extraction process. Local shape features of an image can be represented by histogram function of all subregion. As mentioned in Step 1, Edge contours were computed and gradients of all regions have been estimated using Sobel Mask with size of 3 x 3 without Gaussian smoothing.

Step 4: Finally, the HOG vectors of all pyramid has been normalized and concatenated, which represents the spatial information of the input image. Also, different level of pyramid can be characterized by different size of vectors. That is level 0 is represented by a K vector based on K bins of the histogram. Similarly level 1 is represented by 4K vector.

If the image is having the size of l then the PHOG descriptor based feature dimensionality is represented by $K \sum_{i=L}^l 4^i$ (4)

2.2 Classification

2.2.1 Parslets

We use the idea of partlets to characterize a library of pretrained part detectors that are trained by attractive advantage of the technology of midlevel visual elements detection [30]–[32] in a weakly supervised learning scheme where only image class labels are required. The trained partlets are responsible to identify discriminative visual elements and then to estimate a visual elements-oriented image representation. This new meth of image representation can be fetch best features and content of an image, making this effectively identify a challenging land-use task in image classification.

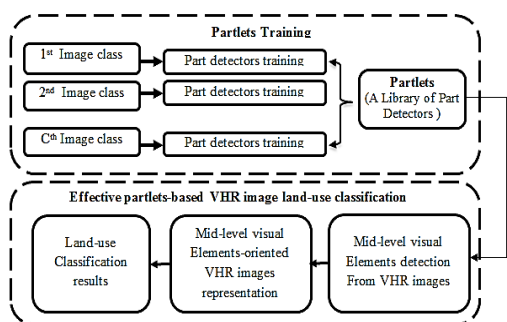


Fig 3. Partlets based Land-use classification

Fig. 3 gives a summary of the partlets-based land-use classification technique. It is mostly consist of two stages, i.e., training of partlets and land-use classification. In first stage, all images from database are undergone training by, Pyramid HOG features [25], and image clustering of similar patch, appearance and pixel values. Then, partlets is formed by concatenating part detector of all image classes. In the second stage, we first execute the trained partlets to identify discriminative visual elements from all images. Then, we characterize the image by calculating its response to partlets. Lastly, we accomplish classification by using a simple linear SVM classifier.

2.2.2 Sparselets

A. Overview

Sparselets were first presented by Song et al. [33] as a new shared intermediate representation for improving speedy process in multiclass object detection. In general, Sparselets are generic dictionary of $D = [d_1, d_2, \dots, d_K] \in \mathfrak{R}^{m \times K}$ trained from a number of parlets (Part Detector) $= [F_1, F_2, \dots, F_N] = [\omega_1, \omega_2, \dots, \omega_N] \in \mathfrak{R}^{m \times K}$ (To simplify the equlation , n = bias tem is neglected)

, where each column $d_k \in \mathfrak{R}^m$ ($k=1,2,..K$), is named as “Sparselets”. Where K = the dictionary size and N denotes the number of partlets. With $N = \sum_{c=1}^C J_c$.

Let ψ denotes the pyramid HOG features of an image. Sparse linear combination of sparselets D by given by,

$$\psi^* F_i \approx \psi^* (D \alpha_i) = \psi^* (\sum_{k=1}^K \alpha_{ik} d_k) = \sum_{k=1}^K \alpha_{ik} (\psi^* d_k) \quad (5)$$

Where $\alpha_i = [\alpha_{1k}, \alpha_{2k}, \dots, \alpha_{iK}]^T \in \mathfrak{R}^K$ is an activation vector of each detector F_i .

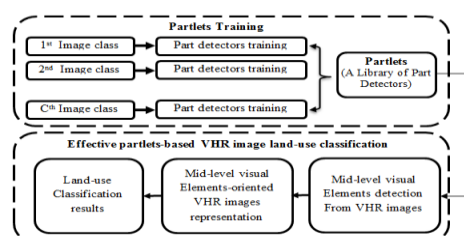


Fig 4. Overview of Sparselets for land-use classification

Fig. 4 gives a summary of the sparselets-based land-use classification method, which contains of two stages, i.e., training of sparselets and classification of land-use area. In the first stage, library of partlets is used to train the sparselets. In the next stage of land-use classification, first the sparselets response of all images are calculated and partlets response is combined with it to form discriminative vectors for classification. Lastly, images are characterized and classified by using the similar way as the partlets-based land-use classification method. B.Coarse sparselets training The proposed coarse sparselets training is illustrated in Fig.5, which is based on unsupervised single-hidden-layer auto-encoder (SA), and Algorithm 1.

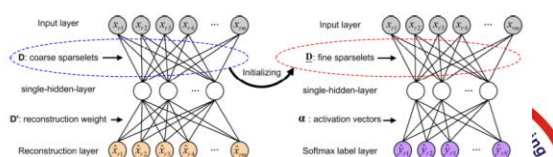


Fig 5. System model for coarse to fine sparselets training

If we have N part detectors $W = [w_1, w_2, \dots, w_N] \in \mathfrak{R}^{m \times N}$ and each detector has n vectors attained from training set used for parlets training, the PHOG feature is an input of the SA with Nnm dimensional while we use N parlets for support to avoid over-fitting. Let $X = [x_1, x_2, \dots, x_{Nn}] \in \mathfrak{R}^{m \times Nn}$ denote the Nn input data, $x_r = [x_{r1}, x_{r2}, \dots, x_{rnm}]^T \in \mathfrak{R}^m$ ($r = 1, 2, \dots, Nn$) denote an m -dimensional PHOG feature vector of each detection and $\hat{x}_r = [\hat{x}_{r1}, \hat{x}_{r2}, \dots, \hat{x}_{rnm}] \in \mathfrak{R}^m$ denote the reconstruction of x_r . our objective is to learn $D = [d_1, d_2, \dots, d_K] \in \mathfrak{R}^{m \times K}$ and $D' = [d'_1, d'_2, \dots, d'_K] \in \mathfrak{R}^{m \times K}$ to make the output of the restoration layer to be as similar to the input layer as possible, i.e., $\hat{x}_r \approx x_r$ by minimizing the following objective function $F_1(D, D', x)$ with activation sparsity constraint to hidden layer:

$$F_1(D, D'; x) = \frac{1}{2Nn} \sum_{r=1}^{Nn} \|x_r - \hat{x}_r\|_2^2 + \beta \sum_{k=1}^K KL(\rho \|\hat{\rho}_k), \quad (6)$$

$$\hat{x}_r = \frac{D'}{1 + \exp(-D'^T x_r)} \quad (7)$$

$$KL(\rho \|\hat{\rho}_k) = \rho \log \frac{\rho}{\hat{\rho}_k} + (1 - \rho) \log \frac{1 - \rho}{1 - \hat{\rho}_k} \quad (8)$$

$$\hat{\rho}_k = \frac{1}{Nn} \sum_{r=1}^{Nn} (1 + \exp(-d_k^T x_r))^{-1} \quad (9)$$

where D is the to-be-learned coarse sparselets with its elements subjected to $\|d_k\|_2 = 1$ ($k = 1, 2, \dots, K$), D' is restored weight matrix used to rebuild the input layer from the hidden layer, K is the number of neurons in the hidden layer which based to the sparselets dictionary size, the weight of the sparsity penalty is denoted by β , ρ is the target hidden nodes, and the average activation of the k -th hidden node over the Nn training data is represented by $\hat{\rho}_k$. The Kullback-Leibler divergence $KL(\cdot)$ is a typical function for computing how dissimilar two distributions are, which delivers the sparsity limitation. Here we set $\beta = 3$ and $\rho = 0.05$ as recommended in [34].

Equation (4) shows that the measures of an average rebuilding error between the input data x_r and the reconstructed data \hat{x}_r .

If the model attains a good rebuilding using D and D' , we can be sure that the trained sparselets have conserved most of the information of partlets. In fact, we solve this optimization problem by using the L-BFGS algorithm [35] which enables to discourse large-scale data with limited memory. Details of this result can be found in numerous connected works [34].

C. Fine sparselets and discriminative activation vectors training

This is to notice that we have a numerous training examples with confident part detector labels. In order to integrate this features to suitably exploit the discriminative features hidden in the training examples, we introduce to additional fine-tune the trained coarse sparselets to expand their simplification capability and concurrently train discriminative activation vectors in a combined frame work, by building a supervised single-hidden-layer neural network (SNN), as demonstrated in Fig. 5(b) and Algorithm 2. In the meantime, to make the trained activation vectors to be discriminative and sparse, we

introduce to enhance a new objective function by imposing L0-norm sparsity limit on the discriminative vectors.

Alteration from reconstruction layer of Fig. 5(a), the output layer is act as a binary vector with a softmax unit that permits 1 for one element out of N -dimensions for N -way classification issues. The fine sparselets are now not only trained from reconstructing the input data, but also from a softmax classifier calculating the labels. A discriminative objective function calculates an average classification loss between the actual label, $y_r = [y_{r1}, y_{r2}, \dots, y_{rN}]^T \in \mathfrak{R}^N$ and the predicted label $[\hat{y}_{r1}, \hat{y}_{r2}, \dots, \hat{y}_{rN}] \in \mathfrak{R}^N$ by imposing L0-norm sparsity limit on the activation vectors, the new discriminative objective function $F_2(D, \alpha; x, y)$ shall be rephrased as:

$$F_2(D, \alpha; x, y) = \frac{1}{2Nn} \sum_{r=1}^{Nn} \|y_r - \hat{y}_r\|_2^2 + Z(\alpha) \quad (10)$$

$$\hat{y}_r = \text{softmax}(\alpha D^T x_r), \quad (11)$$

$$Z(\alpha) = \frac{1}{2} \sum_{i=1}^N \|\alpha_i\|_2^2 \quad \text{s.t. } \|\alpha_i\|_0 \leq \lambda, \forall i = 1, 2, \dots, N \quad (12)$$

Where $D = [d_1, d_2, \dots, d_K] \in \mathfrak{R}^{m \times K}$ is the to-be-trained fine sparselets with its elements exposed to $\|d_k\|_2 = 1$ ($k = 1, 2, 3, \dots, K$), α is the to-be-trained discriminative activation vectors, γ is represented as weight decay parameter limits the significance of the two terms which is set to be 0.001 as recommended in [36], λ is the nonzero element's counts in each activation vector, and $\text{softmax}(a_i) = \exp(a_i) / \sum_i \exp(a_i)$ ($i = 1, 2, 3, \dots, N; a \in \mathfrak{R}^N$).

New objective function of (9) defines; the first term is a supervised goal confirming the learned sparselets to be made fine difference between different part detectors. The second term is an optimization term that tends to decrease the magnitude of the activation vectors and helps to prevent over-fitting, while with L0-norm limit to attain sparsity. Alike to coarse sparselets training, we resolve this over fitting issue by using the L-BFGS algorithm [35]. Though, as the second term is an NP-hard over fitting problem, we accept a similar solution as [37] to roughly decrease it by employing a two-step process. To be exact, in the first step, based on the learned coarse sparselets D , we adjust the activation vectors α by decreasing the average rebuilding error between all part detectors and their reconstruction estimation via the following equation:

$$\min \frac{1}{N} \sum_{i=1}^N \|w_i - D \alpha_i\|_2^2 \quad \text{s.t. } \|\alpha_i\|_0 \leq \lambda, \forall i = 1, 2, \dots, N \quad (13)$$

In our proposed work, we use the OMP algorithm [36] executed in the SParse Modeling Software (SPAMS) package [36] to enhance Eq. (12). In the next step, the initialization of nonzero variables is fixed, which leads to the satisfaction of the sparsity limits and results in a convex over fitting problem to solve. We then train the certain variables discriminatively according to (9).

III. RESULTS AND DISCUSSION

3.1 Experimental Result

Fig 6 and Fig 7 illustrated the input image and classification



map of our proposed method respectively. In the map, four diverse land-use categories have been classified, that's represented by different color. In Fig 7, the city outline could be well differentiated, and few false classifications were made between city and natural areas. One can appreciate the benefits of hybrid feature extraction with Sparselets to find maps that comprehensively identify all measured land uses: there are no mis- or unclassified area as Fig 7.

Preprocessed Image



Classified image



Fig 6. Input Image and Fig 7. Land-Use Classification

3.2 Performance Comparison

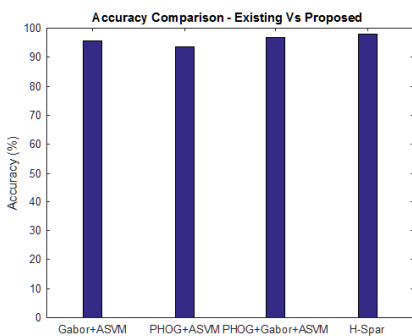


Fig 8 Classification result of Different Classifier

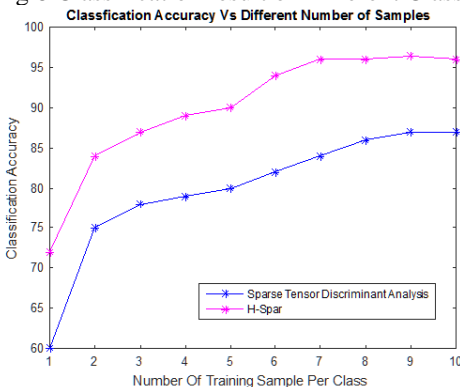


Fig 9 Comparison of classifier in terms of number of samples

Fig 8 illustrates that classification result achieved by different feature extraction techniques. In particular, hybrid PHOD with SPCA outperformed when using the proposed

framework of Sparselets. Gabor + Adaboost + SVM method presents 95.652% of accuracy. Maximum accuracy is achieved by PHOG+Gabor+ Adaboost+SVM [38] as 96.739%. But, in our proposed method yields better performance than [38] by hybrid feature extraction in land-use classification. Fig 9 shows the classification accuracy performance for the existing method with our H-Spar. This is to be noticed that our proposed method has the best performance among the Sparse Tensor Discriminant Analysis [39] in terms of accuracy.

IV. CONCLUSION

In this paper, a hybrid feature extraction of SPCA and PHOG is discussed with a new framework of sparselet (H-Spar) to enhance efficient in land-use classification. In feature extraction segment, The PHOG features with minimum feature vectors were extracted from land-use image, which leads to dimensionality reduction in feature space. And in SPCA, by imposing l_1 limit on regression coefficients for resolving the optimal issue through elastic net, these sparse based techniques provided advantages in both interpretability and classification ability. Furthermore, fine sparselets and feature vectors were together and concurrently learned in a unified framework by building a supervised single-hidden-layer neural network and to prevent over fitting a new discriminative objective function with L0-norm sparsity limit, making the data hidden in the learning samples to be exploited effectively. Experimental results show that the proposed coarse-to-fine learning framework opens a new window for future subsequent improvement of sparselets work, showing sparselets-based methods' enormous potential for quick and accurate in land-use recognition tasks.

REFERENCES

1. G. Cheng et al., "Automatic landslide detection from remote-sensing imagery using a scene classification method based on BoVW and pLSA," *Int. J. Remote Sens.*, vol. 34, no. 1, pp. 45–59, Jan. 2013.
2. A. M. Cheriadat, "Unsupervised feature learning for aerial scene classification," *IEEE Trans. Geosci. Remote Sens.*, vol. 52, no. 1, pp. 439–451, Jan. 2014.
3. Y. Yang and S. Newsam, "Bag-of-visual-words and spatial extensions for land-use classification," in *Proc. ACM SIGSPATIAL Int. Conf. Adv. Geograph. Inf. Syst.*, 2010, pp. 270–279.
4. Y. Yang and S. Newsam, "Spatial pyramid co-occurrence for image classification," in *Proc. IEEE Int. Conf. Comput. Vis.*, 2011, pp. 1465–1472.
5. H. Li, H. Gu, Y. Han, and J. Yang, "Object-oriented classification of high resolution remote sensing imagery based on an improved colour structure code and a support vector machine," *Int. J. Remote Sens.*, vol. 31, no. 6, pp. 1453–1470, Mar. 2010.
6. X. Huang, L. Zhang, and L. Wang, "Evaluation of morphological texture features for mangrove forest mapping and species discrimination using multispectral IKONOS imagery," *IEEE Geosci. Remote Sens. Lett.*, vol. 6, no. 3, pp. 393–397, Jun. 2009.
7. N. Longbotham et al., "Very high resolution multiangle urban classification analysis," *IEEE Trans. Geosci. Remote Sens.*, vol. 50, no. 4, pp. 1155–1170, Apr. 2012.
8. Y. Chen, N. M. Nasrabadi, and T. D. Tran, "Hyperspectral image classification via kernel sparse representation," *IEEE Trans. Geosci. Remote Sens.*, vol. 51, no. 1, pp. 217–231, Jan. 2013.
9. S. Moustakidis, G. Mallinis, N. Koutsias, J. B. Theodoridis, and V. Petridis, "SVM-based fuzzy decision trees for classification of high spatial resolution remote sensing images," *IEEE Trans. Geosci. Remote Sens.*, vol. 50, no. 1, pp. 149–169, Dec. 2012.



10. J. Munoz-Mari, D. Tuia, and G. Camps-Valls, "Semisupervised classification of remote sensing images with active queries," *IEEE Trans. Geosci. Remote Sens.*, vol. 50, no. 10, pp. 3751–3763, Sep. 2012.
11. D. Tuia, M. Volpi, M. Dalla Mura, A. Rakotomamonjy, and R. Flamary, "Automatic feature learning for spatio-spectral image classification with sparse SVM," *IEEE Trans. Geosci. Remote Sens.*, vol. 52, no. 10, pp. 6062–6074, Oct. 2014.
12. G. Cheng, J. Han, P. Zhou, and L. Guo, "Multi-class geospatial object detection and geographic image classification based on collection of part detectors," *ISPRS J. Photogramm. Remote Sens.*, vol. 98, pp. 119–132, Dec. 2014.
13. S. Bhagavathy and B. S. Manjunath, "Modeling and detection of geospatial objects using texture motifs," *IEEE Trans. Geosci. Remote Sens.*, vol. 44, no. 12, pp. 3706–3715, Dec. 2006.
14. M. Kim, M. Madden, and T. A. Warner, "Forest type mapping using object-specific texture measures from multispectral Ikonos imagery: segmentation quality and image classification issues," *Photogramm. Eng. Remote Sens.*, vol. 75, no. 7, pp. 819–829, Jul. 2009.
15. X. Zheng, X. Sun, K. Fu, and H. Wang, "Automatic annotation of satellite images via multifeature joint sparse coding with spatial relation constraint," *IEEE Geosci. Remote Sens. Lett.*, vol. 10, no. 4, pp. 652–656, Jul. 2013.
16. B. Fernando, E. Fromont, and T. Tuytelaars, "Mining mid-level features for image classification," *Int. J. Comput. Vis.*, vol. 108, no. 3, pp. 186–203, Jul. 2014.
17. F. F. Li and P. Perona, "A Bayesian hierarchical model for learning natural scene categories," in *Proc. IEEE Int. Conf. Comput. Vis. Pattern Recog.*, 2005, pp. 524–531.
18. D. G. Lowe, "Distinctive image features from scale-invariant keypoints," *Int. J. Comput. Vis.*, vol. 60, no. 2, pp. 91–110, Nov. 2004.
19. S. Lazebnik, C. Schmid, and J. Ponce, "Beyond bags of features: Spatial pyramid matching for recognizing natural scene categories," in *Proc. IEEE Int. Conf. Comput. Vis. Pattern Recog.*, 2006, pp. 2169–2178.
20. L. Zhang, X. Zhen, and L. Shao, "Learning object-to-class kernels for scene classification," *IEEE Trans. Image Process.*, vol. 23, no. 8, pp. 3241–3253, Jun. 2014.
21. F. Zhu and L. Shao, "Weakly-supervised cross-domain dictionary learning for visual recognition," *Int. J. Comput. Vis.*, vol. 109, no. 1/2, pp. 42–59, Aug. 2014.
22. N. Dalal and B. Triggs, "Histograms of oriented gradients for human detection," in *IEEE Computer Society Conference on Computer Vision and Pattern Recognition*, vol. 1, pp. 886–893, June 2005.
23. Jin Wang, Ping Liu, "Human Action recognition based on pyramid histogram of oriented gradients," pp. 2449–2454, 2009.
24. A.J. Calder, A.M. Buton, P. Miller, A.W. Young and S. Akamatsu, "A principal component analysis of facial expression," *Vision Research*, vol. 41, pp. 1179–1208, April 2001.
25. Yang Bai, Lihua Guo, "A novel feature extraction method using pyramid histogram of orientation gradients for smile recognition", *ICIP 2009*, pp. 3305–3308, 2009.
26. H. Zou and T. Hastie, "Regularization and variable selection via the elastic net," *Journal of Royal Statistical Society. Series B, Statistical Methodology*, Vol. 67, no. 2, pp. 301–320, 2005.
27. A. Bosch, A. Zisserman, and X. Munoz, "Representing shape with a spatial pyramid kernel", in *Proceedings of the International Conference on Image and Video Retrieval*, pp. 401–408, 2007.
28. S. Lazebnik, C. Schmid, and J. Ponce, "Beyond bags of features: Spatial pyramid matching for recognizing natural scene categories", in *IEEE Computer Society Conference on Computer Vision and Pattern Recognition*, vol. 2, pp. 2169–2178, 2006.
29. N. Dalal and B. Triggs, "Histograms of oriented gradients for human detection", in *IEEE Computer Society Conference on Computer Vision and Pattern Recognition*, vol. 1, pp. 886–893, June 2005.
30. Q. Li, J. Wu, and Z. Tu, "Harvesting mid-level visual concepts from large scale Internet images," in *Proc. IEEE Int. Conf. Comput. Vis. Pattern Recog.*, 2013, pp. 851–858.
31. C. Doersch, A. Gupta, and A. A. Efros, "Mid-level visual element discovery as discriminative mode seeking," in *Proc. Conf. Adv. Neural Inf. Process. Syst.*, 2013, pp. 494–502.
32. S. Singh, A. Gupta, and A. A. Efros, "Unsupervised discovery of mid-level discriminative patches," in *Proc. Eur. Conf. Comput. Vis.*, 2012, pp. 73–86.
33. H. O. Song et al., "Sparselet models for efficient multiclass object detection," in *Proc. Eur. Conf. Comput. Vis.*, 2012, pp. 802–815.
34. A. Ng, "CS294A lecture notes: Sparse autoencoder," Stanford Univ., Stanford, CA, USA, 2010.
35. J. Han et al., "Background prior based salient object detection via deep reconstruction residual," *IEEE Trans. Circuits Syst. Video Technol.*, to be published.
36. N. Dalal, and B. Triggs, "Histograms of oriented gradients for human detection," in *Proc. IEEE Int. Conf. Comput. Vis. Pattern Recog.*, 2005, pp. 886–893.
37. R. Girshick, H. O. Song, and T. Darrell, "Discriminatively activated sparselets. In *ICML*, 2013.
38. Yang Bai, Lihua Guo, Lianwen Jin, "A Novel Feature Extraction Method Using Pyramid Histogram Of Orientation Gradients For Smile Recognition", in *IEEE*, 2009.
39. Lu Wang ; Xiaoming Xie; Wei Li ; Qian Du ; Guojun Li, "Sparse feature extraction for hyperspectral image classification", *Signal and Information Processing (ChinaSIP)*, 2015 *IEEE China Summit and International Conference* on 12-15 July 2015.

AUTHORS PROFILE

Author-1
Photo

P. Dolphin Devi Vice Principal, Kalvi Matriculation Higher Secondary School, Oddanchatram, Dindigul - 624612

Author-2
Photo

Dr. K. Chitra Professor, Department of computer science, Government Arts College Melur, Madurai, India